Solitary waves in Bragg gratings with a quadratic nonlinearity

T. Peschel, U. Peschel, and F. Lederer*
Institut für Festkörpertheorie und Theoretische Optik, Friedrich-Schiller-Universität, Max-Wien-Platz 1, D-07743 Jena, Germany

B. A. Malomed
Department of Applied Mathematics, School of Mathematical Sciences, Tel Aviv University, Ramat Aviv 69978, Israel
(Received 21 August 1996)

We study the formation of solitary waves in quadratic nonlinear materials where the dispersion is provided by linear mode coupling mediated by a Bragg grating. We show that solitary wave solutions can be analytically found provided that the coupling of the second-harmonic waves considerably exceeds that of the fundamental ones. Furthermore, we numerically determine solitary wave solutions for the general case. These solutions prove to be close to the analytical ones. A nontrivial property of Bragg grating solitary waves is that they do not fill the complete parameter space where exponentially decaying functions are allowed to exist. Instead, we find internal boundaries inside this parameter space where the soliton intensity diverges. Moreover, double-hump solutions are found where a numerical propagation procedure shows that some of them are fairly robust. [S1063-651X(97)03404-1]

PACS number(s): 42.65.Tg, 42.65.Ky

I. INTRODUCTION

The study of temporal and spatial solitons [or solitary waves (SW's)] is among the fascinating subjects of nonlinear optics. They represent a stable and robust equilibrium state in time or space that is due to the balance of linear dispersion or diffraction and nonlinear phase modulation. Hence the nature of solitary waves is determined by the interplay between the linear and nonlinear properties of the environment. As far as the linear properties are concerned the anomalous group velocity dispersion (GVD) of optical fibers made from fused silica [1] or the diffraction taking place in planar waveguide structures [2] can be exploited. Most recently, it has been shown that the huge anomalous dispersion required for temporal SW formation in a short channel waveguide can be achieved by a proper waveguide tailoring [3]. There is another option left to generate a large GVD in configurations where material dispersion merely plays a marginal role, viz., the linear coupling of two modes with dissimilar group velocities as it occurs in an asymmetric waveguide coupler [4] or in Bragg gratings [5].

With regard to the nonlinearity induced phase modulation the traditional approach is based on the instantaneous cubic (Kerr) nonlinearity as far as nonresonant nonlinearities are concerned. If this specific nonlinearity arises in any of the dispersive or diffractive configurations various solitons or SW's have been shown to exist as, e.g., temporal [1] and spatial Schrödinger solitons [2] or Bragg grating SW's [5].

During the past several years materials with large instantaneous, quadratic nonlinearities have attracted a great deal of interest. It has been shown that the phase modulation, which appears simultaneously to the amplitude modulation in the consecutive up and down conversion process, may even balance the self-diffraction of a beam in a planar waveguide [6] or in a bulk material [7] leading to the formation of SW's where the fundamental frequency (FF) and the second-harmonic (SH) frequency beams are mutually trapped. There is a bundle of theoretical papers [8–19] where the explicit shape of these types of SW's, their stability and collision behavior are studied provided that diffraction or dispersion can be described in the parabolic approximation. In order to generate temporal SW's a control of both the phase and group velocities of FF and SH waves has to be achieved simultaneously. However, in most realistic materials the group-velocity mismatch cannot be compensated and a detrimental temporal walk-off between the FF and SH wave occurs. One opportunity to overcome this problem exists in exploiting the huge dispersion that is due to the mode coupling in Bragg gratings. So, there is, on the one hand, a practical need to look for SW solutions in that configuration, but, on the other hand, the search for these solutions is of fundamental interest, too.

In cubic nonlinear materials these SW solutions have been theoretically studied for many years (see [20] and the references therein, [21,22]) and experimentally proven to exist lately [5]. It is now well understood that these SW's can be excited close to the linear photonic band gap. The SW solutions exhibit a large chirp [22], which guarantees that the frequency of the low intensity tails is located within the gap preventing the coupling to the linear radiation.

A first attempt to study Bragg grating SW's in a quadratic nonlinearity was made in [23]. However, this paper dealt only with the limit of large phase mismatch where the originally quadratic nonlinearity degenerates to a cubic one and the familiar SW solutions [20–22] appear. Evidently, in restricting to this particular limit one misses the genuine effects evoked by the quadratic nonlinearity that are expected to show up close to phase matching. But more importantly, the SW solutions found for that particular limit are not compatible with the original equations that we are going to show later.

We have yet to mention that switching and bistability in Bragg gratings with a quadratic nonlinearity were investi-

*Electronic address: pfl@physik.uni-jena.de

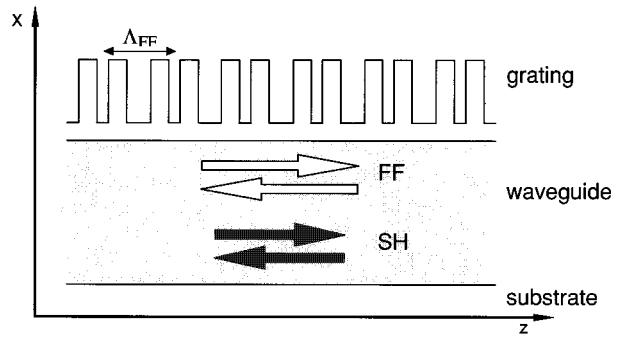

FIG. 1. Schematic of a double periodic grating that mediates the coupling of forward and backward propagating modes at the FF and the SH frequency (Λ_{FF}: grating period).

gated numerically [24]. There the emphasis was not paid to SW solutions because the grating-induced dispersion for the SH wave was neglected.

The objective of the present work is a systematic analysis of SW solutions in quadratic nonlinear materials where the dispersion is generated by a Bragg grating mediated coupling of forward and backward propagating modes. The paper is structured as follows. In Sec. II we derive the basic set of equations describing the dynamics of the field envelopes in the configuration under investigation. Then we discuss the requirements and constraints for bright SW solutions to exist.

In Sec. III we develop an approximate model that represents the natural ''cubic'' limit and allows for analytical solutions. It is based on the assumption that the linear coupling between both SH waves considerably exceeds that between the FF waves.

Eventually we use numerical means to solve the basic system of equations. We compare the domains where SW solutions may exist with that found in the approximate model. Furthermore, we study in detail a few of the SW solutions and check their robustness by propagating them numerically.

II. THE BASIC EQUATIONS

We consider forward and backward propagating modes in a waveguide at both the FF and the SH. These modes shall be coupled by a Bragg grating that is etched into the cladding layer of an approximately phase-matched waveguide (see Fig. 1). This corresponds, likewise, to an effective index grating. The fundamental grating period is Λ_{FF}. The respective grating vector is given by $K_B=2\pi/\Lambda_{FF}$. The grating is designed such that forward and backward propagating FF waves are just coupled by this vector. Obviously, the SH waves are then coupled by the second Fourier component of the grating that is twice the grating vector. Usually the corresponding coupling efficiency is less than that for the FF waves. If required, it can be enhanced by introducing a substructure, e.g., another groove, into each unit cell as shown in Fig. 1.

Evidently, the FF Bragg grating may cause radiation losses for the SH. These losses can be suppressed by an appropriate design of the grating shape. Another loss mechanism for the FF wave can be attributed to the so-called Cherenkov SH generation where the SH wave leaves the waveguide in a direction perpendicular to the waveguide surface. These losses are important for fairly thin waveguides only. In the following we will neglect both loss mechanisms as well as absorption and assume that both the FF and the SH modes are guided.

The complete optical field is given as a superposition of forward and backward propagating fields at both frequencies as

$$\begin{aligned}\vec{E}(\vec{Y},Z,T)=&[E_+^{\mathrm{FF}}(Z,T)e^{(i/2)K_BZ-i(\Omega_B+\Omega)T}\\&+E_-^{\mathrm{FE}}(Z,T)e^{-(i/2)K_BZ-i(\Omega_B+\Omega)T}]\vec{f}_{\mathrm{FF}}(\vec{Y})\\&+[E_+^{\mathrm{SH}}(Z,T)e^{iK_BZ-2i(\Omega_B+\Omega)T}\\&+E_-^{\mathrm{SH}}(Z,T)e^{-iK_BZ-2i(\Omega_B+\Omega)T}]\vec{f}_{\mathrm{SH}}(\vec{Y})+\text{c.c.},\end{aligned}\tag{1}$$

where T is the time and $\vec{Y}$ denotes the transverse coordinates. It is convenient to separate fastly oscillating terms, which are related to the grating (Bragg) vector K_B of the FF grating, with the period Λ_{FF} and to the respective Bragg frequency Ω_B in the center of the linear band gap. Ω_B serves as a reference frequency whereas the actual frequency of the solution is given by $\Omega_B+\Omega$. The grating vector K_B is determined by the period of the FF grating Λ_{FF} and shall obey the Bragg condition for the propagation constant of the FF mode $K(\Omega)$ at the Bragg frequency. Hence we have

$$K_B=\frac{2\pi}{\Lambda_{\mathrm{FF}}}\quad\text{and}\quad 2K(\Omega_B)=K_B.$$

Moreover, we have introduced the slowly varying envelopes $E_{+/-}^{\mathrm{FF/SH}}(Z,T)$ and the vectorial mode profiles $\vec{f}_{\mathrm{FF/SH}}$. In the framework of the coupled-mode approach these profiles are determined for an averaged (with respect to the propagation direction) profile and do not change upon propagation. The nonlinearly induced polarization shall not be influenced by the grating and is determined by the field profiles $\vec{f}_{FF/SH}$ only. The additional polarization induced by the grating results in a coupling between forward and backward propagating waves. Typically the waveguides are only a few centimeters long and the pulses are in the picosecond regime. Hence we can assume the group velocities V_{FF} and V_{SH} of the fundamental and second-harmonic waves to be constant in the frequency domain under consideration. Consequently, higher-order dispersion is neglected.

The resulting equations of motion for the slowly varying envelopes of the optical fields ($E_{+/-}^{\mathrm{FF/SH}}$) read now as (for a more detailed derivation see, e.g., [1] Chap. 10.6.3., pp. 451–459; [20] Chap. 3.3, pp. 212–217 [25,26])

$$0=\left[i\,\frac{1}{V_{\mathrm{FF}}}\,\frac{\partial}{\partial T}+i\,\frac{\partial}{\partial Z}+\frac{\Omega}{V_{FF}}\right]E_+^{\mathrm{FF}}+\kappa_{\mathrm{FF}}E_-^{\mathrm{FF}}+\chi_{\mathrm{eff}}(E_+^{\mathrm{FF}})^*E_+^{\mathrm{SH}},\tag{2a}$$

$$0=\left[i\,\frac{1}{V_{\mathrm{FF}}}\,\frac{\partial}{\partial T}-i\,\frac{\partial}{\partial Z}+\frac{\Omega}{V_{\mathrm{FF}}}\right]E_-^{\mathrm{FF}}+\kappa_{\mathrm{FF}}^*E_+^{\mathrm{FF}}+\chi_{\mathrm{eff}}(E_-^{\mathrm{FF}})^*E_-^{\mathrm{SH}},\tag{2b}$$

$$0=\left[\frac{i}{V_{\mathrm{SH}}}\frac{\partial}{\partial T}+i\frac{\partial}{\partial Z}+K(2\Omega_B)-K_B+\frac{2\Omega}{V_{\mathrm{SH}}}\right]E_+^{\mathrm{SH}}+\kappa_{\mathrm{SH}}E_-^{\mathrm{SH}}+\chi_{\mathrm{eff}}(E_+^{\mathrm{FF}})^2, \tag{2c}$$

$$0=\left[\frac{i}{V_{\mathrm{SH}}}\frac{\partial}{\partial T}-i\frac{\partial}{\partial Z}+K(2\Omega_B)-K_B+\frac{2\Omega}{V_{\mathrm{SH}}}\right]E_-^{\mathrm{SH}}+\kappa_{\mathrm{SH}}^{*}E_+^{\mathrm{SH}}+\chi_{\mathrm{eff}}(E_-^{\mathrm{FF}})^2, \tag{2d}$$

where χ_{eff} is the effective nonlinear coefficient of the waveguide. The coupling coefficients κ_{FF} and κ_{SH} are proportional to the first and second Fourier components of the grating. In general they are complex valued. One phase can be removed by a simple phase transformation but the ratio $\kappa_{\mathrm{SH}}/\kappa_{\mathrm{FF}}$ is left complex. This phase may lead to qualitative changes of the respective SW solutions. But the phase vanishes for gratings with mirror-symmetric unit cells. For the sake of clarity and simplicity we restrict ourselves to that case and assume this ratio to be positive.

Then we may further reduce the number of free parameters of the solution by a proper normalization as

$$z=\kappa_{\mathrm{FF}}Z,\quad t=V_{\mathrm{FF}}\kappa_{\mathrm{FF}}T,$$

$$U_{+/-}=\frac{\chi_{\mathrm{eff}}}{\kappa_{\mathrm{FF}}}E_{+/-}^{\mathrm{FF}},\quad V_{+/-}=\frac{\chi_{\mathrm{eff}}}{\kappa_{\mathrm{FF}}}E_{+/-}^{\mathrm{SH}},$$

$$q=\frac{K(2\Omega_B)-K_B}{\kappa_{\mathrm{FF}}},\quad \kappa=\frac{\kappa_{\mathrm{SH}}}{\kappa_{\mathrm{FF}}},\quad \omega=\frac{\Omega}{\kappa_{\mathrm{FF}}V_{\mathrm{FF}}},\quad v_0=\frac{V_{\mathrm{SH}}}{V_{\mathrm{FF}}},$$

where κ is the scaled coupling constant. The scaled wave-vector mismatch and the ratio of the group velocities at the Bragg frequency are denoted by q and v_0, respectively. The normalized equations of motion for the amplitudes at the FF ($U_{\pm}$) and the SH ($V_{\pm}$) read now as

$$0=\left[i\frac{\partial}{\partial t}+i\frac{\partial}{\partial z}+\omega\right]U_++U_-+U_+^{*}V_+, \tag{3a}$$

$$0=\left[i\frac{\partial}{\partial t}-i\frac{\partial}{\partial z}+\omega\right]U_-+U_++U_-^{*}V_-, \tag{3b}$$

$$0=\left[\frac{i}{v_0}\frac{\partial}{\partial t}+i\frac{\partial}{\partial z}+q+\frac{2}{v_0}\omega\right]V_++\kappa V_-+U_+^2, \tag{3c}$$

$$0=\left[\frac{i}{v_0}\frac{\partial}{\partial t}-i\frac{\partial}{\partial z}+q+\frac{2}{v_0}\omega\right]V_-+\kappa V_++U_-^2. \tag{3d}$$

Before we proceed with the solution of Eqs. (3), we identify domains where bright solitary waves that moving with a velocity v (scaled with V_{FF}) may exist. A suitable criterion consists in requiring that the tails of these localized objects, where the nonlinearity is negligible, have to decay exponentially for both frequencies. Because we expect that the SW solutions exhibit a chirp we introduce the frequency of the linear tails as the frequency ω (2ω) of the FF (SH) SW's. Now, the existence criterion may be formulated more precisely. Both frequencies ω and 2ω have to be situated within the stop bands of the respective Bragg gratings. Now the linearized version of Eqs. (3) can be used to get the respective domains in the velocity-frequency plane as

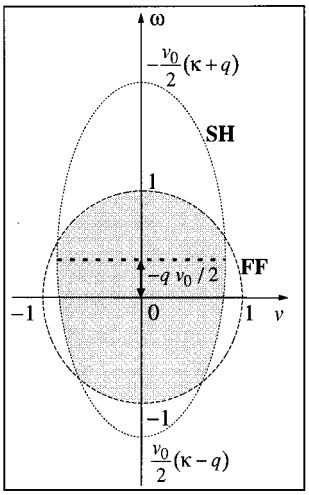

FIG. 2. Maximum range in the velocity-frequency plane where bright solitary waves may exist (shadowed area).

$$\omega^2+v^2<1\quad \text{for the FF} \tag{4a}$$

and

$$\left[\frac{1}{\kappa}\left(q+\frac{2}{v_0}\omega\right)\right]^2+\left(\frac{v}{v_0}\right)^2<1\quad \text{for the SH.} \tag{4b}$$

These conditions define a circular and an elliptic domain where their centers are separated with respect to the ω direction if the wave-vector mismatch q is nonzero (see Fig. 2). The width of the gap for the SH is proportional to the ratio of the coupling constants κ. Evidently, bright solitary waves may exist in the overlap region only (shadowed area in Fig. 2). The wave-vector mismatch, the ratio of the coupling constants and that of the group velocities of the unperturbed waveguide modes determine the size of this region. Because the solutions are expected to be chirped, the averaged frequency of the SW can deviate from the SW frequencies ω (2ω) and need not be situated inside the stop band.

The system of Eqs. (3) can only be solved numerically. But in Sec. III we are going to show that a considerable simplification can be achieved and that analytical solutions can be derived, provided that certain constraints concerning the linear coupling are introduced. Moreover, it will turn out that, at least qualitatively, most of the pertinent features of Bragg grating SW's can be derived from this analytical model.

III. A SIMPLIFIED ANALYTICAL MODEL

The so-called ''Schrödinger limit'' for SW's in uncorrugated quadratic nonlinear media (henceforth termed as ''conventional SW's'') [11–14] is based on the assumption that for large phase mismatch the derivatives in the equation of motion for the SH wave can be omitted. Thus propagation effects with respect to the SH component can be neglected and the SH wave sticks rigidly at the FF wave. Hence both the FF and the SH wave merely experience a phase modulation similar to that in cubic nonlinearities. Unfortunately, the

straightforward extension of this approach to Bragg gratings fails. A large increase of the mismatch evokes a separation of the domains of existence of SW's [see Eqs. (4) and Fig. 2] and prevents them from overlapping. This fact has been overlooked in [23].

However, in inspecting Eqs. (3) we find another option, to neglect propagation effects for the SH wave in Bragg gratings, viz, to increase the ratio of the coupling coefficients κ. This limit requires the coupling between the SH modes to be considerably larger than that between the FF modes. This condition can be easily met by a proper grating design. The modulus of the wave-vector mismatch q must only be smaller than the ratio of the coupling coefficients, but need not be small in general. In using the simplified system of equations, one has to keep in mind that the domains of existence of SW's are defined by Eqs. (4), i.e., optional solutions outside the overlap region are meaningless. In particular, this concerns the SW velocity v, which must not exceed the ratio of the group velocities v_0 [see Eqs. (4)]. We note that the limit of large κ reduces also the scattering losses of the SH evoked by the grating for the FF. Now we neglect the derivatives in the SH part of our basic system (3) and get for the SH, fields

$$V_{+/-}=\frac{-U_{-/+}^2+\Delta U_{+/-}^2}{\kappa(1-\Delta^2)}, \tag{5}$$

where we have introduced the effective wave vector mismatch Δ as a function of the SW frequency ω,

$$\Delta=\frac{1}{\kappa}\left(q+\frac{2}{v_0}\,\omega\right). \tag{6}$$

From Eqs. (4) it immediately follows that $\Delta^2<1$ has to hold and consequently from Eq. (5) that the nonlinear cross coupling is the dominant effect. This means that a FF wave in forward direction preferably generates a SH wave, which moves backward and vice versa. Now we substitute Eq. (5) into the first two equations of Eqs. (3) and obtain the simplified system describing the evolution of the FF waves as

$$0=\left[i\,\frac{\partial}{\partial t}+i\,\frac{\partial}{\partial z}+\omega\right]a_+ + a_- - a_+^* a_-^2+\Delta|a_+|^2 a_+\,, \tag{7a}$$

$$0=\left[i\,\frac{\partial}{\partial t}-i\,\frac{\partial}{\partial z}+\omega\right]a_- + a_+ - a_-^* a_+^2+\Delta|a_-|^2 a_-\,, \tag{7b}$$

where we have used the normalization

$$a_{+/-}=\frac{U_{+/-}}{\sqrt{\kappa(1-\Delta^2)}}. \tag{8}$$

The system (7) describes the evolution of the FF fields coupled by a Bragg grating and is subject to an effective third-order nonlinearity. But unlike in the ''Schrödinger limit'' (large mismatch) for conventional SW's [11–14], the evolution equations differ considerably from their ''cubic'' counterpart (Bragg SW's in Kerr media [20–22]). The main difference consists in the dominant role of nonlinear energy exchange that is due to cross coupling. With respect to the normalized FF amplitudes (8), this contribution to the nonlinear response is independent from the size of the wave vector mismatch, but the mismatch still enters via the normalization. Self-phase modulation is only of minor importance because of $|\Delta|<1$. Like in the Schrödinger limit for conventional SW's, self-phase modulation appears only if the effective wave-vector mismatch is nonzero. Here, its strength varies with the SW frequency. Cross-phase modulation does not appear at all whereas in Kerr media it is twice as strong as the self-phase modulation. The simplified system of Eqs. (7) exhibits three integrals of motion that represent the pulse energy E, the Hamiltonian H, and the pulse momentum P, respectively,

$$E=\int_{-\infty}^{\infty}[|a_+|^2+|a_-|^2]dz, \tag{9a}$$

$$H=\frac{1}{2}\int_{-\infty}^{\infty}\left[i\left(a_+^*\,\frac{\partial a_+}{\partial z}-a_-^*\,\frac{\partial a_-}{\partial z}\right)+\omega(|a_+|^2+|a_-|^2)+2a_+a_-^*-a_+^2a_-^{*2}+\frac{\Delta}{2}\,(|a_+|^4+|a_-|^4)\right]dz+\text{c.c.}, \tag{9b}$$

$$P=\frac{i}{2}\int_{-\infty}^{\infty}\left[a_+^*\,\frac{\partial a_+}{\partial z}+a_-^*\,\frac{\partial a_-}{\partial z}\right]dz+\text{c.c.} \tag{9c}$$

We look for stationary solitary waves moving with the velocity v:

$$a_{+/-}(z,t)=\tilde{a}_{+/-}(x) \quad \text{with} \quad x=z-vt. \tag{10}$$

The resulting ordinary differential equations read as

$$0=\left[i(1-v)\,\frac{\partial}{\partial x}+\omega\right]\tilde{a}_+ + \tilde{a}_- - \tilde{a}_+^*\tilde{a}_-^2+\Delta|\tilde{a}_+|^2\tilde{a}_+\,, \tag{11a}$$

$$0=\left[-i(1+v)\,\frac{\partial}{\partial x}+\omega\right]\tilde{a}_- + \tilde{a}_+ - \tilde{a}_-^*\tilde{a}_+^2+\Delta|\tilde{a}_-|^2\tilde{a}_-\,. \tag{11b}$$

They exhibit two integrals of motion for the amplitudes $A_{+/-}(x)=|\tilde{a}(x)|$ and phases $\sigma_{+/-}(x)=\arg(\tilde{a}(x))$:

$$\tilde{E}=(1-v)A_+^2-(1+v)A_-^2 \tag{12}$$

and

$$\tilde{H}=\omega(A_+^2+A_-^2)+2A_+A_-\cos(\psi)-A_+^2A_-^2\cos(2\psi)+\frac{\Delta}{2}\,(A_+^4+A_-^4), \tag{13}$$

which are related to the conserved quantities E and H of system (7), respectively. Here we have introduced the phase difference $\psi(x)=\varphi_+(x)-\varphi_-(x)$.

Using the integrals of motion $\tilde{E}$ and $\tilde{H}$ we solve the system (11) by a procedure similar to that outlined in [22]. Our

approach differs in that we focus on the phase evolution first and then use the conservation laws to get explicit expressions for the intensity.

For bright SW's being of concern here both conserved quantities equate to zero for arbitrary x. Because of $\widetilde{E}=0$ we may introduce an effective intensity as

$$I=(1-v)A_+^2=(1+v)A_-^2. \tag{14}$$

Moreover, $\widetilde{H}=0$ can be used to express the intensity in terms of the phase difference $\psi(x)$,

$$I=2\sqrt{1-v^2}\,\frac{\sigma+\cos(\psi)}{2\cos^2(\psi)-1-\delta}, \tag{15}$$

where we have introduced

$$\sigma=\omega/\sqrt{1-v^2} \tag{16}$$

and

$$\delta=\Delta(1+v^2)/(1-v^2). \tag{17}$$

Obviously the constraint (4) imposed on the FF wave implies $-1<\sigma<1$ whereas the modulus of the detuning parameter δ may exceed unity although $|\Delta|<1$ holds.

We have to determine the phase difference $\psi(x)$. By inserting Eqs. (10), (14), and (15) into the evolution equations (7), we end up with the differential equation

$$\frac{d\psi}{dx}=-\frac{2}{\sqrt{1-v^2}}\,[\sigma+\cos(\psi)]. \tag{18}$$

Depending on the initial conditions [$\psi_1(0)=0$ or $\psi_2(0)=\pi$] we get the respective solutions

$$\psi_1(x)=-2\arctan\left\{\left(\frac{1+\sigma}{1-\sigma}\right)^{1/2}\tanh\left[x\left(\frac{1-\sigma^2}{1-v^2}\right)^{1/2}\right]\right\}, \tag{19a}$$

$$\psi_2(x)=\pi+2\arctan\left\{\left(\frac{1-\sigma}{1+\sigma}\right)^{1/2}\tanh\left[x\left(\frac{1-\sigma^2}{1-v^2}\right)^{1/2}\right]\right\}. \tag{19b}$$

For obvious reasons we term ψ_1 and ψ_2 in-phase or antiphase solutions, respectively. As expected, the asymptotic behavior of the phase difference [$\psi(\pm\infty)=\mp\arccos(-\sigma)$] entails vanishing intensities for $x=\pm\infty$ because of Eq. (15).

It is worth mentioning that Eq. (18) likewise holds for a genuine Kerr nonlinearity and any ratio between self- and cross-phase modulation, i.e., the phase difference between forward and backward propagating waves in various Bragg systems does not depend on the specific type of the cubic nonlinearity. On the contrary, the relation between the phase difference and the intensity is critically affected by the form of the cubic nonlinearity. In particular, in the Kerr case, Eq. (15), reads as $I\sim[\sigma+\cos(\psi)]$.

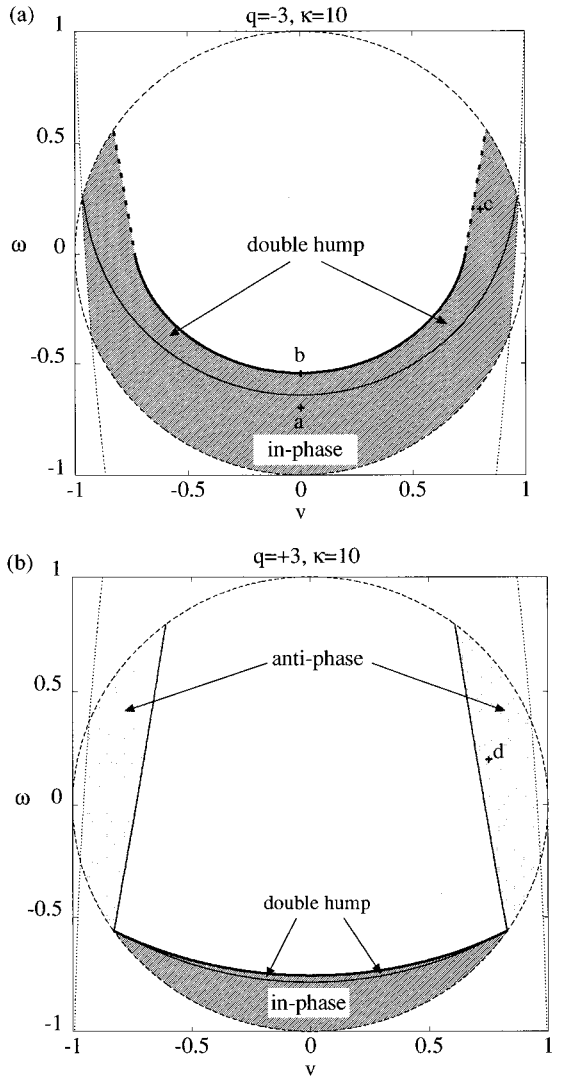

FIG. 3. Domain of existence of SW's derived from the analytical model ($v_0=1$), (a) negative mismatch, (b) positive mismatch (thick solid line, singularity characterized by $|\delta|<1$; thick dashed line, singularity characterized by $|\delta|>1$; thin solid line within the shadowed area, separates single from double-hump solutions; crosses, the locations of the solitary waves shown in the next figure).

Eventually, the phases are determined from the phase difference by an additional integration and we get

$$\varphi_\pm(x)=\pm\frac{\psi(x)}{2}+\frac{\omega v}{1-v^2}\,x + \begin{cases} -\dfrac{2\delta v\,\operatorname{arctanh}\left(\dfrac{1+\delta}{\sqrt{1-\delta^2}}\tan(\psi(x))\right)}{(1-v^2)\sqrt{1-\delta^2}} & \text{for } |\delta|<1 \\ \dfrac{2\delta v\arctan\left(\dfrac{1+\delta}{\sqrt{\delta^2-1}}\tan(\psi(x))\right)}{(1-v^2)\sqrt{\delta^2-1}} & \text{for } |\delta|>1. \end{cases} \tag{20}$$

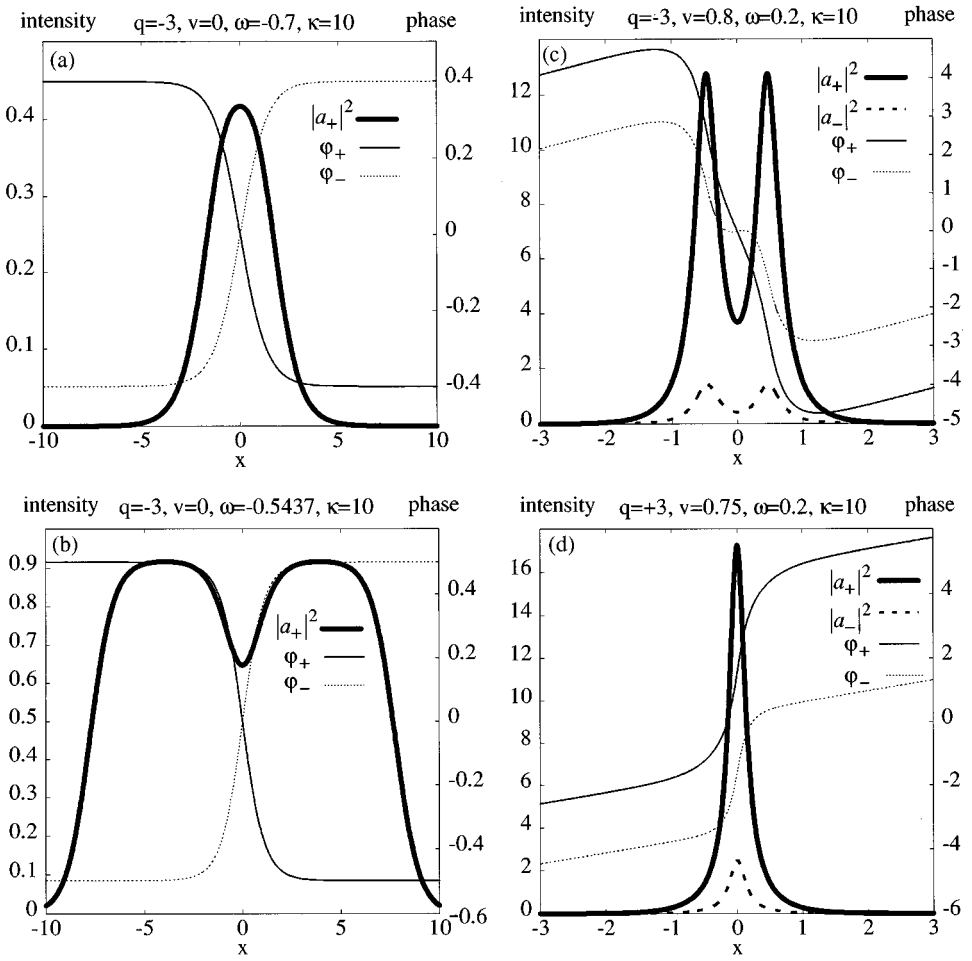

FIG. 4. Shapes of different types of SW's derived from the analytical model ($v_0=1$); (a) in-phase single hump, (b) in-phase double-hump near a boundary with $|\delta|<1$, (c) in-phase double-hump near a boundary with $|\delta|>1$, and (d) antiphase.

Now, in the framework of the approximation used here the solitary wave solutions are completely determined by Eqs. (15), (19), and (20) keeping in mind the normalization (8) and the relation between the FF and SH waves Eq. (5). It is evident that the SW solutions exhibit a chirp familiar from the Bragg grating SW's in cubic materials [22].

A necessary condition for bright SW's to exist is given by Eq. (4), which was derived from linear arguments. Now the question arises if this condition is sufficient or if there are additional constraints in the velocity-frequency plane imposed by the particular form of the nonlinearity. To find this out we primarily make use of Eqs. (15) and (19). The intensity distribution is completely determined by the cosine of the phase differences. From Eq. (19) we get that any SW solution covers the entire range of the respective phase difference given by

$$-\sigma<\cos(\psi_1(x))\leqslant 1, \tag{21a}$$

$$-1\leqslant\cos(\psi_2(x))<-\sigma. \tag{21b}$$

Obviously $\omega(x)$ corresponds only to a permitted solution if the intensity (15) is positive and does not exhibit singularities. We have to distinguish between the two cases $\delta<1$ or $\delta>1$ that will lead to in-phase or antiphase solutions, respectively.

1. $\delta<1$ (in-phase solutions)

The denominator in Eq. (15) is always positive at the boundaries $\cos\psi=\pm 1$ [see condition (21)]. Hence $\cos(\psi)>-\sigma$ is required, which implies an *in-phase solution* $\psi_1(x)$, Eqs. (21). Two cases have to be distinguished with respect to $\delta<1$.

(a) $\delta<-1$. Here, there are no singularities and bright SW's may exist for all frequencies and velocities situated in the domain defined by Eqs. (4) provided that $\delta<-1$ holds.

(b) $-1<\delta<1$. In this case singularities may occur and to have solutions exist requires $\sigma<-\sqrt{(1+\delta)/2}<0$.

2. $\delta>1$ (antiphase solutions)

For the *antiphase solution* $\psi_2(x)$, Eq. (19b), the denominator in Eq. (15) is always negative and consequently there are no singularities.

The domains corresponding to both cases are uniquely defined (see Fig. 3). In particular, regions in the frequency-velocity plane applying to in-phase or antiphase solutions do not overlap. For $|\delta|>1$, self-phase modulation can compare to the energy exchange [see Eqs. (17a) and (7)]. Because the sign of self-phase modulation depends on the sign of the detuning parameter δ, one may expect self-focusing for $\delta>1$ and self-defocusing for $\delta<-1$. As a matter of fact, the antiphase solutions emerging for $\delta>1$ resemble conventional Bragg grating SW's known from self-focusing Kerr nonlinearities [20–22]. However, significant differences from the Kerr case can be identified for the in-phase solutions ($\delta<-1$). We will come back to this issue below. Note that the detuning parameter $|\delta|$ can only become large if the soli-

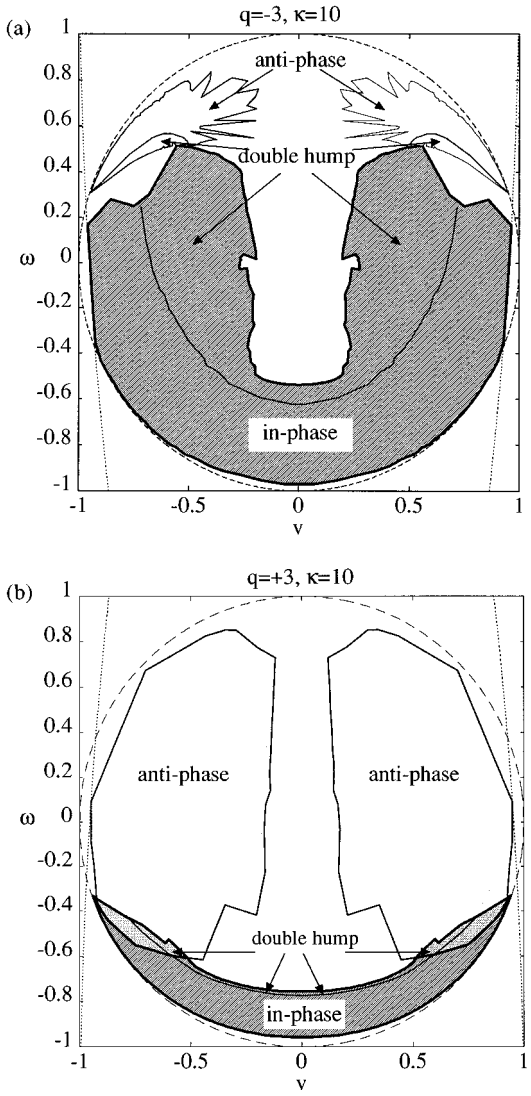

FIG. 5. Numerically determined domain where bright SW solutions of the complete system can exist; (a) negative mismatch and (b) positive mismatch, same parameters as in Fig. 3, $\kappa=10$, $v_0=1$.

ton velocity is not too small [see Eq. (17a)] because $|\Delta|<1$ has to hold.

Domains where SW's can exist are displayed for both negative [Fig. 3(a)] and positive wave-vector mismatch q [Fig. 3(b)]. As already mentioned, we can distinguish between in-phase [Fig. 4(a)] and antiphase solutions [Fig. 4(d)]. In contrast to conventional Bragg grating SW's [20–22] the domain where SW's may exist does not fill the whole area defined by the overlap of the FF and the SH gap [see Eqs. (4)]. Here internal boundaries emerge where the intensity diverges. A physical reason for these singularities may be derived from the fact that at these points the different nonlinear contributions to the Hamiltonian cancel each other exactly. This decrease of the effective nonlinearity requires higher intensities for the SW's to survive leading eventually to the singularities. By using Eq. (17a) the internal boundaries can be determined and are given by

$$\delta=-1 \quad \text{with} \quad \omega>0 \quad \text{for the case 1a,} \tag{22a}$$

$$\sigma=-\sqrt{(1+\delta)/2} \quad \text{for the case 1b} \tag{22b}$$

and

$$\delta=1, \tag{22c}$$

respectively.

Another internal boundary arises from the fact that the intensity as a function of the phase difference (15) may attain a maximum at $|\cos(\psi)|<1$ for certain sets of parameters. This leads to the generation of a double-hump SW for in-phase solutions [Figs. 4(b) and 4(c)] provided that

$$\sigma>-\frac{3+\delta}{4} \tag{23}$$

holds.

If the SW parameters (v and ω) approach the internal boundaries the intensity (15) at a certain x tends to diverge and the shape of SW's changes dramatically. The nature of these changes depends on the type of the internal boundary and on the point x where the intensity touches the divergence. Two different scenarios can be distinguished (see Fig. 3).

(1) If $|\delta|<1$ holds [case 1b (22b)] we have a double-hump in-phase solution [see Eq. (23)] in the vicinity of the internal boundary. The denominator of Eq. (15) reaches its minimum at the boundaries of ψ [see Eq. (21)] or in the wings of the SW at $x=\pm\infty$. Consequently the intensity in the tails increases as the pulse width does likewise. The shape in the pulse center resembles a gray soliton [see Fig. 4(b)].

(2) In contrast, for $|\delta|>1$ the singularity appears for finite x. Hence the peak intensity increases to infinity and correspondingly the width decreases if the SW parameters approach an internal boundary. Again in-phase solutions exhibit a double-hump shape. Very close to the boundary the distance between the humps remains constant while the peaks shrink and the SW practically splits into two parts [see Fig. 4(c)]. Obviously, in cases where the width of the SW shrinks considerably the basic assumption of our analytical model that the nonlinearity acts locally becomes invalid. Hence near the internal boundaries the solutions of the analytical model have to be double-checked by the numerical solution of the basic system (3).

IV. SOLITARY WAVES—THE GENERAL CASE

In Sec. III analytical solutions of the simplified system (7), which holds for a strong coupling of the SH waves or correspondingly a quasilocal nonlinear response, were studied in detail. Now we are going to numerically solve the complete set of basic equations (3). The aim is twofold, viz., to check the reliability of the analytical solutions and to search for new SW's if we lift the requirement of strong coupling and local response. To this end we used a Newton iteration scheme where the analytical solutions served as initial conditions.

For strong coupling of the SH waves ($\kappa=10$) a reasonable agreement with the previous results could be established (compare Figs. 3 and 5). Both in-phase [see Fig. 6(a)] and antiphase solutions [see Fig. 6(b)] could be identified even for large velocities where the analytical approach is not strictly valid. Although the allowed parameter ranges are larger than predicted by our model they do not fill the gap

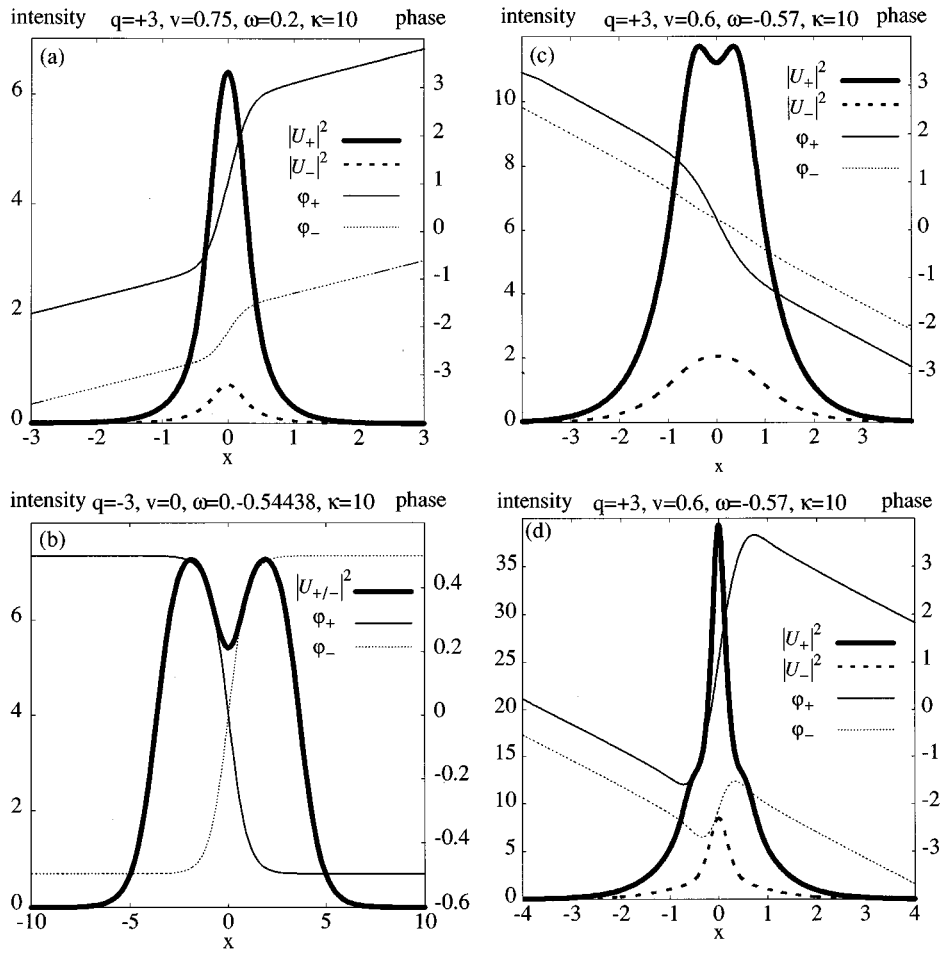

FIG. 6. Different types of numerically determined SW solutions ($v_0=1$), (a) antiphase solution corresponding to Fig. 4(d), (b) in-phase solution corresponding to Fig. 4(b), (c) bistable SW (in-phase), and (d) bistable SW (antiphase).

completely. The existence of internal boundaries within the gap where the solutions diverge could be confirmed. Double-hump solutions were found in the parameter ranges predicted by the analytical model (see Fig. 6). The physical picture provided by the analytical model seems to be even more general than expected. Even for large velocities or weak coupling of the SH waves ($\kappa=1$) the essential behavior of the solutions described above remains unchanged (see Fig. 7). But, on the other hand, it is not surprising that the diversity of the SW solutions of the complete system is richer than predicted by the analytical model. The parameter range where antiphase solutions with nonvanishing velocities occur considerably exceeds the analytically predicted one. Even for a mismatch where antiphase solutions must not exist in the analytical model they were found numerically [compare Figs. 3(a) and 5(a)]. As far as double-hump SW's are concerned antiphase solutions could be additionally identified [see Figs. 5(a) and 7]. Moreover, it turned out that SW's with multiple humps may appear and that the SH field is no longer proportional to the FF field if both coupling constants compare (see Fig. 8).

The strict separation between in-phase and antiphase solutions could be essentially confirmed by the numerical studies without regard to a small overlap region [see Fig. 5(b)]. Within this region both in-phase and antiphase solutions exist simultaneously and give rise to bistability [see Figs. 6(c) and 6(d)].

To check the robustness of the unconventional double-hump solutions some of them were propagated numerically. No decay could be found for negative SW frequencies, even if we used an approximate analytical solution as initial distribution. In that case long-lived internal oscillations emerged around the exact stationary solution. Two different oscillating modes could be identified. The antisymmetric mode can be related to an exchange between the peak intensities whereas the breathing of the field shape can be attrib-

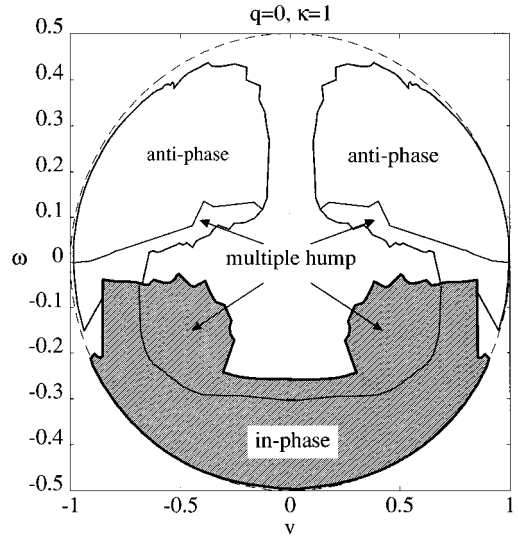

FIG. 7. Numerically determined domain for SW solutions if the coupling strength of FF and SH waves are equal ($\kappa=1$, $v_0=1$).

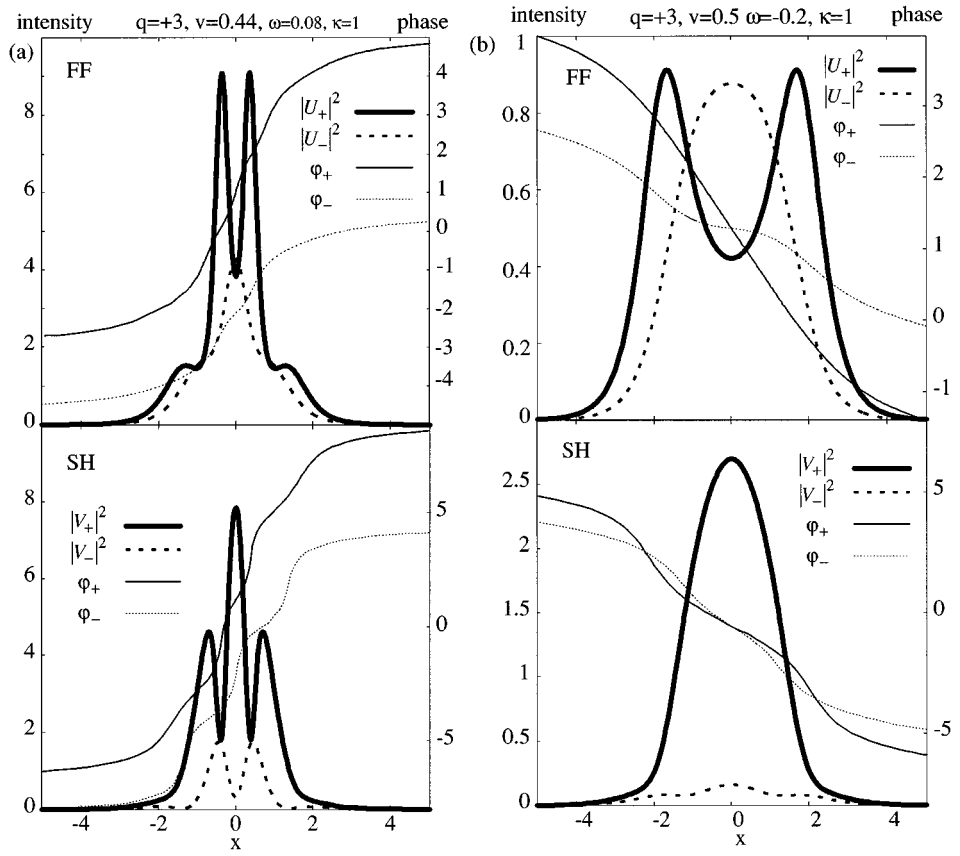

FIG. 8. Numerically determined multiple-hump solutions for equal coupling of FF and SH ($v_0=1$), (a) antiphase solution and (b) in-phase solution.

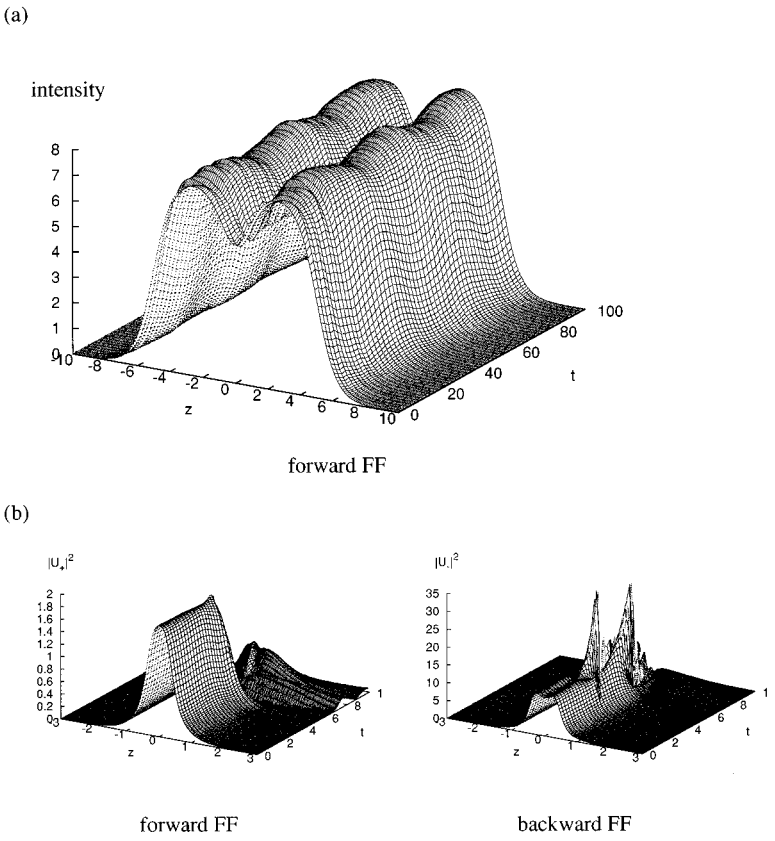

FIG. 9. Propagation of double-hump SW's, (a) stable propagation, an approximate analytical solution was taken as the initial shape [same parameters as Fig. 4(b)], and (b) decay of an unstable solution ($\kappa=10$, $q=-3$, $v=-0.7$, $\omega=0.2$).

uted to the symmetric-mode [see Fig. 9(a)].

The situation changes dramatically if positive SW frequencies are concerned. We observed a rapid decay of the double-hump solutions where this decay might be due to the growth of the antisymmetric mode [see Fig. 9(b)].

V. CONCLUSIONS

We have shown that solitary waves consisting of mutually locked FF and SH components can exist in waveguides made from quadratic nonlinear materials. The dispersion required for their existence can be mimicked by linear coupling in a Bragg grating. It turned out that an analytical solution can be found provided that the coupling constant for the SH waves considerably exceeds that for the FF waves. In this case the SH waves are slaved by the FF ones corresponding to a quasilocal nonlinearity. The resulting equations resemble that for the Kerr nonlinearity but with no cross-phase modulation and energy exchange exceeding the self-phase modulation. This simplified model yields a good qualitative description of the behavior of SW's in a quadratic nonlinear environment. The major results of this model could be confirmed by direct numerical integration of the complete system of equations. In contrast to conventional Bragg grating SW's in a cubic nonlinearity, we found internal boundaries within the domain where SW's are expected to exist. These internal boundaries separate regions where SW's may or must not exist. Moreover, additional boundaries mark the transition from single- to double-hump solutions where some of them are stable. Far from the exponential tails all solutions exhibit a chirp. With regard to the phase difference between forward and backward propagating FF waves in the center of the SW's, both in-phase and antiphase solutions occur. They correspond to SW in cubic materials with defocusing or a focusing cubic nonlinearity, respectively. These two different types may even share parts of the parameter space thus giving rise to bistability.

Eventually, we mention that the model derived here as well as the basic equations and results likewise hold for a configuration where the dispersion is provided by the coupling of copropagating modes with different group velocities as it appears in asymmetric directional couplers [4].

ACKNOWLEDGMENTS

We acknowledge a grant from the Deutsche Forschungsgemeinschaft in the framework of the Sonderforschungsbereich 196.

[1] G. P. Agrawal, *Nonlinear Fiber Optics*, 2nd ed. (Academic, San Diego, 1995).
[2] J. S. Aitchison, A. M. Weiner, Y. Silberberg, M. K. Oliver, J. L. Jackel, D. E. Leaird, E. M. Vogel, and P. W. E. Smith, Opt. Lett. **15**, 471 (1990).
[3] C. J. Hamilton, B. Vögele, J. S. Aitchison, G. T. Kennedy, W. Sibbet, W. Biehlig, U. Peschel, T. Peschel, and F. Lederer, Opt. Lett. **21**, 1226 (1996).
[4] U. Peschel, T. Peschel, and F. Lederer, Appl. Phys. Lett. **67**, 2111 (1995).
[5] B. J. Eggleton, R. E. Slusher, C. M. de Sterke, P. A. Krug, and J. E. Sipe, Phys. Rev. Lett. **76**, 1627 (1996).
[6] R. Schiek, Y. Baek, and G. I. Stegeman, Phys. Rev. E **53**, 1196 (1996).
[7] W. E. Torruellas, Z. Wang, D. J. Hagan, E. W. Van Stryland, and G. I. Stegeman, Phys. Rev. Lett. **74**, 5036 (1995).
[8] Y. N. Karamzin and A. P. Sukhorukov, Pis'ma Zh. Eksp. Teor. Fiz. **20**, 734 (1974) [JETP Lett. **20**, 339 (1974)].
[9] M. J. Werner and P. D. Drummond, J. Opt. Soc. Am. B **10**, 2390 (1993).
[10] K. Hayata and M. Koshiba, Phys. Rev. Lett. **71**, 3275 (1993).
[11] R. Schiek, J. Opt. Soc. Am. B **10**, 1848 (1993).
[12] C. R. Menyuk, R. Schiek, and L. Torner, J. Opt. Soc. Am. B **11**, 2434 (1994).
[13] L. Torner, Opt. Commun. **114**, 136 (1995).
[14] L. Torner, C. R. Menyuk, and G. Stegeman, J. Opt. Soc. Am. B **12**, 889 (1995).
[15] A. V. Buryak and Y. S. Kivshar, Phys. Lett. A **197**, 407 (1995).
[16] A. V. Buryak, Y. S. Kivshar, and V. V. Steblina, Phys. Rev. A **52**, 1670 (1995).
[17] D. E. Prelinkovsky, A. V. Buryak, and Y. S. Kivshar, Phys. Rev. Lett. **75**, 591 (1995).
[18] L. Torner, D. Mihalache, D. Mazilu, and N. N. Akhmediev, Opt. Lett. **20**, 2183 (1995).
[19] C. Etrich, U. Peschel, B. Malomed, and F. Lederer, Phys. Rev. A **52**, R3444 (1995).
[20] C. M. de Sterke and J. E. Sipe, in *Progress in Optics*, edited by E. Wolf (Elsevier, Amsterdam, 1994), Vol. XXXIII, p. 203.
[21] A. B. Aceves and S. Wabnitz, Phys. Lett. A **141**, 37 (1989).
[22] J. Feng and F. K. Kneubühl, IEEE J. Quantum Electron. **QE-29**, 590 (1993).
[23] Yu. S. Kivshar, Phys. Rev. E **51**, 1613 (1995).
[24] M. Picciau, G. Leo, and G. Assanto, J. Opt. Soc. Am B **13**, 661 (1996).
[25] H. G. Winful, J. H. Marburger, and E. Garmire, Appl. Phys. Lett. **35**, 379 (1979).
[26] U. Trutschel, U. Langbein, F. Lederer, and H. Ponath, IEEE J. Quantum Electron. **QE-21** 1639 (1985).